Astron. Astrophys. 327, 493–502 (1997)

ASTRONOMY
AND
ASTROPHYSICS

Millimetre line CO (2→1) observations of a complete sample of AGN

D. Rigopoulou[1,2,3], **I. Papadakis**[4], **A. Lawrence**[1,5], **and M. Ward**[6]

[1] Physics Department, Queen Mary and Westfield College, University of London, Mile End Road, London E1 4NS, UK
[2] MPE für Extratterestrische Physik, Postfach 1603, D-85740 Garching, Germany
[3] Astrophysics Group, Blackett Laboratory, ICSTM, Prince Consort Road, London SW7 2BZ, UK
[4] Physics Department, University of Southampton, University Road, Southampton, UK
[5] Edinburgh Institute for Astronomy, Royal Observatory Edinburgh, Blackford Hill, Edinburgh EH9 3HJ, UK
[6] Department of Physics and Astronomy, University of Leicester, Leicester LE1 7RH, UK

Received 24 February 1997 / Accepted 17 June 1997

Abstract. We report on observations of the CO (2→1) transition of a complete subset of 11/39 of the Piccinotti (1982) hard X-ray selected AGN sample. All of the 11 galaxies were clearly detected. All the galaxies in our sample are strong hard-X ray sources and thus the sample is unbiased with respect to obscuring material. Six of the galaxies are Seyfert 1 type objects with the rest five being reddened Seyfert 1s, or the so called "Narrow Line Galaxies". Based on our high S/N detections we investigate the relation between CO and far-infrared luminosities. A strong correlation is found to exist for both Seyfert 1s and Narrow Line Galaxies similar to the one seen in normal and bright infrared galaxies. Our data also suggest that the FIR emission in Seyferts galaxies is of thermal origin, an argument which is supported by three different lines of evidence, the CO-FIR correlation, the FIR/M(H_2) dependence on dust temperature and the similarities in the shapes of the CO and HI profiles. The relation between CO emission and non-thermal radio power was examined next. Seyferts were found to show an excess radio non-thermal power for a given CO luminosity (when compared to starburst galaxies) while no differences were found between Seyfert 1s and 2s in their CO and radio properties (Seyfert 2s were selected from the literature). We conclude that Seyfert 1s and Narrow Line Galaxies have very similar properties with respect to their molecular gas reservoir. By comparing our CO observations with published optical data we explore the distribution of the molecular clouds in the sample galaxies. We find that in most cases the spatial distribution of CO clouds is confined within 1-1.4 kpc around the nucleus.

Key words: galaxies: active – ISM: molecules – galaxies: Seyferts

Send offprint requests to: d.rigopoulou@ic.ac.uk

1. Introduction

Two of the current problems in research on active galaxies concern the mechanism by which the nuclear activity is fuelled and the relationship between the activity and the formation of massive stars. The latter problem is further related to a more fundamental issue concerning the origin of the far-infrared (FIR) emission in AGNs, and whether this is dust re-radiation of starlight or is due to re-radiated emission from the active nucleus (Bregman 1990 and references therein). There are two basic components in the standard picture of AGNs: the "central engine" component, in the form of a putative supermassive black hole, and the "fueling material", the source of gas whose gravitational energy is dissipated via accretion. The origin of the "fueling material" and in particular whether this is intrinsic or extrinsic to the nucleus, is not very clear. Despite earlier suggestions (Telesco et al. 1988, Bregman 1990) that the source of gas is extrinsic to the nucleus, in recent studies of host dynamics in a complete sample of moderate luminosity AGNs (Ho et al. 1997) there is no indication of material being brought into the nucleus from the interstellar medium of the host galaxy.

Millimeter CO observations of Seyfert galaxies aim at giving definite answers to a number of fundamental questions, including those mentioned above. A number of CO observations of individual Seyferts have been made so far, e.g. Rickard et al. (1985), Blitz et al. (1986), Meixner et al. (1990), and Mazzarella et al. (1993). A survey of optically bright Seyferts was carried out by Heckman et al. (1989). A large number of Seyfert 2s were detected, but only 5 Seyfert 1s. According to this survey, Seyfert 1s have smaller CO/FIR ratios than do Seyfert 2s, and the latter appear more like Starbursts with regard to their CO/FIR properties, however, these statistics are only marginal. Furthermore, their results may be biased towards type 1 Seyfert objects, since in optically selected samples only the most luminous Seyfert 2s will be included. Another study of the CO properties

of Seyfert 1s and 2s was recently presented by Maiolino et al. (1997).

In this paper new CO observations of a sample of hard X-ray selected active galaxies (Piccinotti et al. 1982) are presented. The current sample is unbiased with respect to dust, since hard X-rays can penetrate dust more easily than radiation at longer wavelengths, and so it is better suited than most optical samples for studies of the properties of Seyfert 1 and Seyfert 2 galaxies. Moreover, the current sample contains objects which are clearly reddened Seyfert 1s i.e. the so-called "Narrow Line X-ray Galaxies", whose CO/FIR ratio is not well determined. The initial Piccinotti sample contains 39 AGNs. For our present CO sample we selected objects which comply with the following criteria, i) Dec $>$ -40^o (so that they are observable from the JCMT site) and ii) IRAS 60 μm flux density, $S_{60} > 0.5$ Jy (select the brightest targets). The resulting sample consisted of 15 objects, 11 of which where observed and detected with the JCMT. From these 11 galaxies, 6 are type 1 Seyferts and 5 are Narrow Line X-ray Galaxies.

The new observations and data analysis are presented in Sect. 2. In Sect. 3 we deduce molecular hydrogen masses followed by investigation of the CO and FIR relationship in the present sample galaxies. In particular, we investigate the origin of the FIR emission in Seyfert 1 galaxies, discuss the radio-CO correlation and examine possible differences between Seyfert 1 and 2s. Line profiles and the distribution of molecular clouds is discussed in Sect. 4. Finally, our conclusions are summarised in Sect. 5.

Table 1. Observational parameters for the AGN sample.

NAME	R.A. (1950)	Decl. (1950)	redshift (optical)	Int. time (sec)	Keys
(1)	(2)	(3)	(4)	(5)	(6)
MRK 1040 (Sy1)	02 25 16.5	+31 05 18.4	0.0164	2400	H89
NGC 2110 (NLXG)	05 49 46.4	–07 28 01.8	0.0075	2400	H89(U)
MCG 8-11-11 (Sy1)	05 51 09.6	+46 25 51.1	0.0205	3000	H89
NGC 2992 (NLXG)	09 43 17.7	–14 05 42.8	0.0080	1800	BMB86
NGC 3227 (Sy1)	10 20 46.7	+20 07 06.1	0.0038	1500	BMB86
NGC 4151 (Sy1)	12 08 01.0	+39 41 01.0	0.0033	2700	–
NGC 4593 (Sy1)	12 37 04.6	–05 04 11.1	0.0083	1800	H89(U)
NGC 5506 (NLXG)	14 10 39.1	–02 58 26.2	0.0061	1500	H89(U)
NGC 7172 ((NLXG)	21 59 07.3	–32 06 04.0	0.0080	2640	H89
NGC 7314 (NLXG)	22 33 00.4	–26 18 34.9	0.0047	3600	H89(U)
NGC 7469 (Sy1)	23 00 44.4	+08 36 16.1	0.0164	1200	H(89)

Keys to column (6): (U) denotes an upper limit.
H89 Heckman et al. (1989), BMB86 Blitz, et al. (1986)

2. Observations and data analysis

2.1. Observations

Spectral line observations of the CO(2→1) line (v_{rest}=230 GHz) were obtained on the nights of 1993 November 17 and 18, using the James Clerk Maxwell Telescope (JCMT) on Mauna Kea, Hawaii [1], with a single-channel SIS receiver (Receiver A2) together with the Dutch Autocorrelation backend Spectrometer (DAS). The telescope beamsize was 23 arcsec. The SSB noise temperature was 200 K and the total system temperature was 325 K at 230 GHz (Matthews 1992). The DAS configuration provided a bandwidth of 750 MHz with a resolution of 756 kHz. Sky subtraction was performed by azimuth chopping with a throw of 60″ at a frequency of 1 Hz. Spectra were obtained with the velocity centered on the known optical redshifts. The data are presented on a scale of main beam temperature T_{mb} which is appropriate if the source sizes are of the same order as the beam sizes. The main beam efficiency η_{mb} for the JCMT, is equal to 0.63.

[1] The James Clerk Maxwell Telescope is operated by the Royal Observatory, Edinburgh (ROE) on behalf of the United Kingdom Particle Physics and Astrophysics Research Council (PPARC), the Netherlands Organisation for the Advancement of Pure Research (ZWO), the Canadian National Research Council (NRC), and the University of Hawaii (UH).

2.2. Line spectra and intensities

Fig. 1 presents the CO (J = 2→1) spectra for all the objects observed. The ordinate shows the main beam temperature. The redshift range for these galaxies lies between 0.0033 and 0.0205, which is equivalent to velocities of 994 and 6164 km s^{-1} and the peak intensities are between 10 and 138 mK. Of the 11 galaxies detected, 5 of them have previous (1→0) detections (Heckman et al. 1989 and references therein), while for the rest 6 there only exist (1→0) upper limits. Table 1 summarizes the observational parameters: source names and galaxy type (Sy1 for the Seyfert type 1 galaxies and NLXG for the Narrow Line X-ray Galaxies) are listed in column (1); columns (2) and (3) give positions (1950); column (4) optical redshifts; column (5) provides total on-source integration times in seconds; column (6) lists references to CO(1→0) observations from the literature (where available), detections or upper limits. Table 2 summarizes the CO line parameters: source name is listed in column (1); column (2) gives the total CO intensity, I_{CO}, obtained by integrating over the full velocity range; column (3) lists the peak T_{mb} temperature; the optical velocities (expected from the optical redshifts according to which the scans were centered) and centroid velocities from the CO emission are given in columns (4) and (5); column (6) gives the CO line widths at FWHM. The CO line widths were estimated by fitting single or double peak Gaussians to the data.

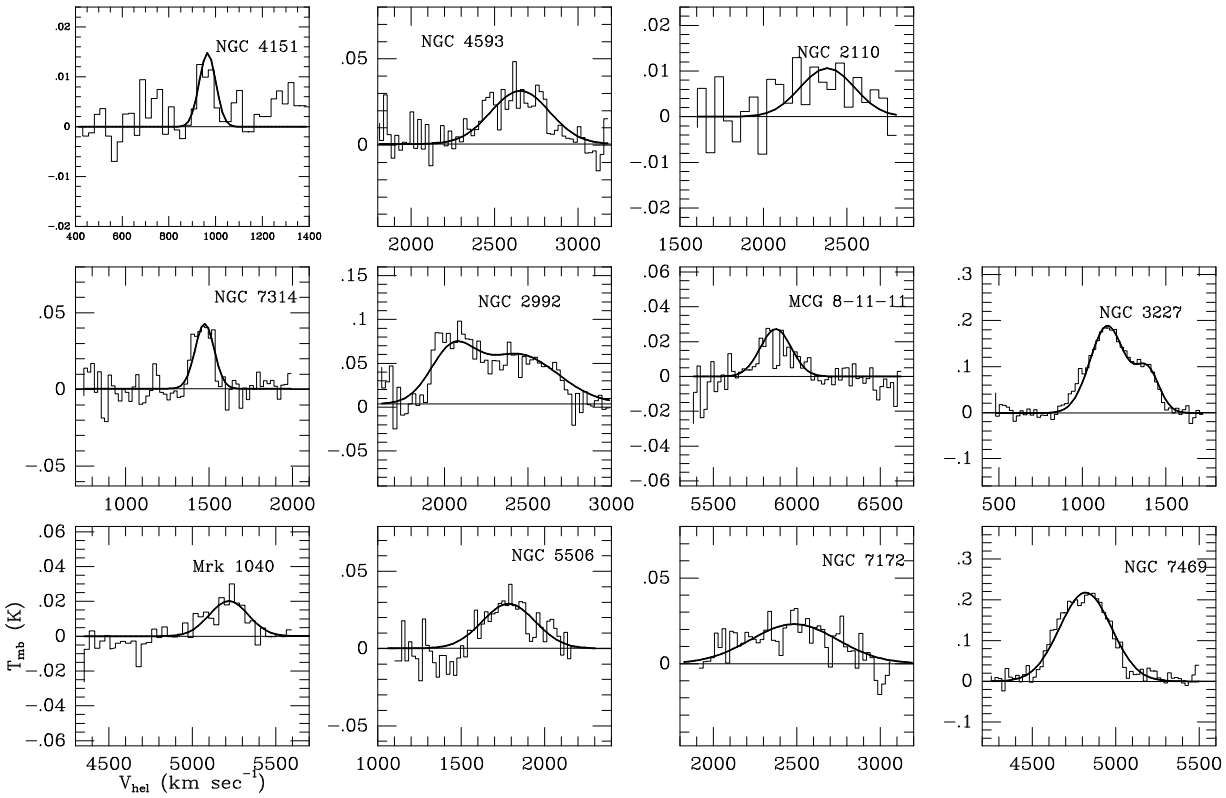

Fig. 1. Line emission profiles of the CO (2→1) emission from 11 hard X-ray selected AGNs. Most spectra have been smoothed to a velocity resolution of 10 km s^{-1}. The intensity scale is in units of T_{mb}. The x-axis is heliocentric velocity v_{hel} expressed in km s^{-1}.

3. Discussion

3.1. Derived quantities

Molecular masses and luminosities were calculated in the same way as in Rigopoulou et al. (1996). To estimate molecular hydrogen masses the conversion factor equal to N(H_2)/mol cm^{-2} = 3×10^{20}(I_{CO}/K km s^{-1}) was used. This value of the conversion factor comes from several empirical methods for clouds in our Galaxy (Scoville et al. 1986, Young & Scoville 1982, Bloemen et al. 1986). Using this conversion factor molecular hydrogen masses were then estimated based on the relationship:

$$M(H_2)[M_\odot] = 4.78 L_{CO}[K\ km\ s^{-1}\ pc^2] \quad (1)$$

where L_{CO} is the CO luminosity measured in K km s^{-1} pc^2. Table 3 lists the derived quantities: column (1) lists names, column (2) distances (assuming H_o = $50 km s^{-1} Mpc^{-1}$), column (3) CO luminosities, column (4) molecular hydrogen mass estimates based on Eq. (1), column (5) L_{IR} luminosities calculated from the 60 and 100 μm IRAS fluxes as described in Helou et al. (1985), column (6) the ratio $L_{IR}/M(H_2)$ and finally column (7) lists the derived dust masses implied by the FIR luminosities, calculated from the expression (by Sanders et al. 1991):

$$\frac{M_{dust}}{[10^4 M_\odot]} = (\frac{L_{FIR}}{10^8 L_\odot})(\frac{40K}{T_{dust}})^5 \quad (2)$$

3.2. CO-FIR correlation and the origin of IR emission

The strong relation between the strength of the CO and FIR continuum in normal and bright infrared galaxies has been the subject of several papers (e.g. Rickard & Harvey 1984, Young et al. 1986, Heckman et al. 1989, Sanders et al. 1991, Rigopoulou et al. 1996). The strong correlation is interpreted as the result of the link between the amount of molecular gas and the rate of star formation. Next, we investigate both the CO-FIR relationship, and the origin of the FIR emission in Seyfert galaxies. We compare their CO properties to those of starburst and Ultraluminous IRAS Galaxies (ULGs), and we investigate possible differences in the CO properties of the various types of active galaxies.

Since our sample contains 11 objects, for the present studies we have included data from the literature as well. The latter data were selected based on two criteria; that the classification of the object is known (ie Seyfert 1 or 2), and that they have been observed in the CO J= 2 → 1 transition using telescopes with known beam efficiencies so that we can correct accordingly for the different beamsizes. The objects from the literature come from the works of the following: (a) Seyferts from Alloin et al. (1992) and Krügel et al. (1992), (b) starbursts from Chini et al. (1992), and Casoli et al. (1992) (both data sets were collected on the IRAM 30m telescope), and (c) Ultraluminous IRAS Galaxies (Rigopoulou et al. 1996), collected on the JCMT 15m telescope. Fig. 2 is a plot of L_{IR} vs M(H_2), including data for all of the abovementioned objects.

Table 2. Line emission parameters.

NAME	Ico* (K km/sec)	Tpeak* (mK)	V_{opt} km/sec	V_{CO} km/sec	ΔV(FWHM) km/sec
MRK 1040	2.6±1.0	22	4927	5201	200
NGC 2110	1.92±0.64	10	2237	2266	320
MCG 8-11-11	4.86±2.02	10	6164	5976	320
NGC 2992[1]	7.88±2.19±1.52	60	2400	2128	219
	14.10±4.03	58	”	2395	403
NGC 3227[1]	22.61±1.52	198	1146	1089	190
	9.1±1.04	95	”	1257	130
NGC 4151	1.56±0.52	20	994	974	130
NGC 4593	4.16±0.78	26	2491	2495	260
NGC 5506	5.13±0.54	32	1815	1765	270
NGC 7172	33.3±1.00	33.3	2400	2410	500
NGC 7314	2.84±0.42	45	1422	1409	110
NGC 7469	39.47±2.86	219	4925	4886	290

* both on “Tmb” scale.
[1] Two Gaussian fits.
Typical rms noise 5 mK.

Table 3. Total Molecular Hydrogen Masses CO and IR Luminosities

NAME other	D (Mpc)	logL_{CO} (K km $s^{-1}pc^2$)	log$M(H_2)$ ($M_\odot$) (empirical)	logL_{IR} $L_\odot$	log($L_{IR}/M(H_2)$) ($L_\odot M_\odot^{-1}$)	T_{dust} K
MRK 1040	98	8.39	8.99	10.61	2.11	36.72
NGC 2110	45	7.58	8.18	10.10	2.12	36.77
MCG 8-11-11	123	8.87	9.49	10.84	1.77	38.32
NGC 2992	48	8.40	9.99	10.44	1.07	34.55
NGC 3227	23	7.92	8.51	9.88	1.54	34.05
NGC 4151	20	6.77	7.38	9.00	1.82	34.00
NGC 4593	50	8.00	8.61	10.12	1.73	34.34
NGC 5506	37	7.83	8.43	10.21	2.11	45.02
NGC 7172	48	8.88	9.49	10.38	1.03	34.23
NGC 7314	28	7.33	7.94	9.85	2.03	31.07
NGC 7469	99	9.57	10.17	11.58	1.58	41.70

Distances calculated assuming H_o = 50$Kms^{-1}Mpc^{-1}$.

It is clear that the CO-FIR relationship for the starbursts and Seyferts (Type 1 and 2 treated as one class) is very similar. We have fitted the starbursts plus ULGs and the Seyferts 1 plus 2 data in Fig. 2 (17 and 18 points in each group respectively) with a linear model of the form $logL_{FIR}$ = A+B[$logM(H_2)-7$], where A is the $logL_{FIR}$ value at $log[M(H_2)]$ = 7 (we have chosen this value for the normalisation in order to minimize the errors on its best fit value), using the least-squares bisector method (Isobe et al. 1990). In the case of starbursts and ULGs the regression is $logL_{FIR}$ = (8.94±0.29)+(0.98±0.11)[$logM(H_2)-7$], while it becomes $logL_{FIR}$ = (8.55±0.19)+(1.11±0.10)[$logM(H_2)-7$] for Seyferts 1 plus 2. The estimated values of A and B are almost identical for the starburst plus ULGs and the Seyferts 1 plus 2 data sets (8.94 ± 0.29, 0.98 ± 0.11 and 8.55 ± 0.19, 1.11 ± 0.10 respectively), suggesting that a similar mechanism (ie dust reradiation of starlight) is responsible for the the CO and FIR emission in all objects. If the dust responsible for emission beyond 40 μm in Seyferts was significantly heated by light produced by processes related to a supermassive black hole one would expect the Seyferts to have systematically an excess FIR luminosity for a given CO luminosity and clearly this is not the case. Furthermore, if a different mechanism were operating in Seyferts (for instance synchrotron from a compact source) then it is difficult to find an explanation for the observed FIR-CO

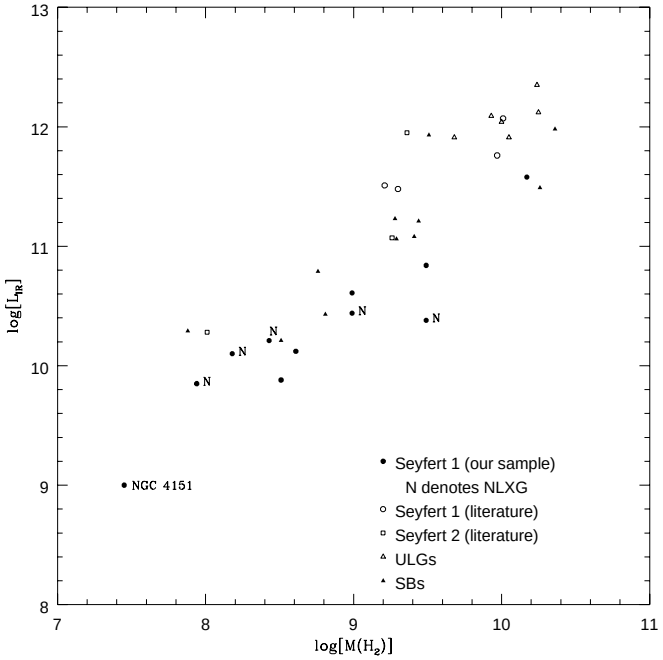

Fig. 2. The infrared luminosity is shown as a function of $M(H_2)$. Solid circles denote Seyfert 1 objects from our sample (the N next to the dot identifies the NLXGs objects of our sample), open circles represent Seyfert 1 type objects from the literature, open squares represent Seyfert 2 objects from the literature, solid triangles are starbursts (from literature) and open triangles are ULGs (from Rigopoulou et al. 1996). The same notation applies to all plots throughout the paper.

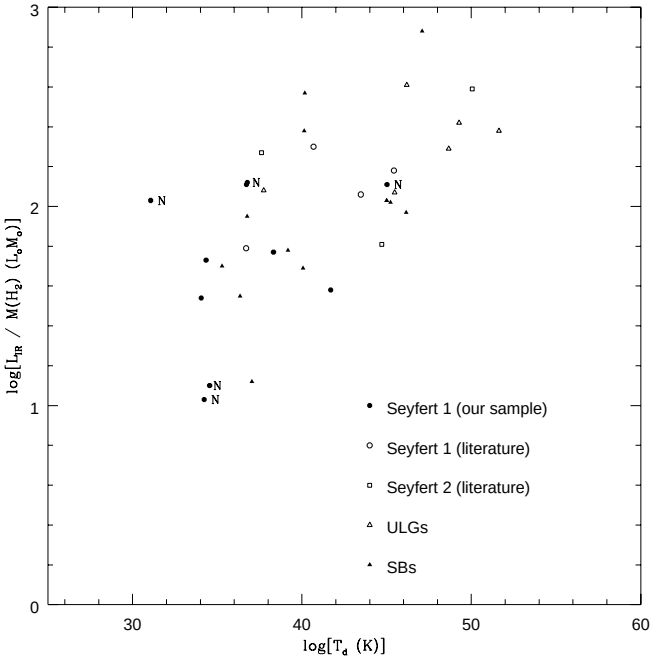

Fig. 3. The ratio L_{IR}/M_{H_2} is shown as a function of the dust temperature. Solid circles are Seyfert 1s from our sample (N denotes the NLXGs), open circles are Seyfert 1s from the literature, open squares are Seyfert 2 from the literature, solid triangles are starbursts and open triangles are ULGs.

luminosity and even more difficult to explain the observed CO emission. A similar conclusion was reached by Heckman et al. (1989) based on the CO ($1 \rightarrow 0$) properties of their sample of Seyfert galaxies. As we mentioned before, our L_{FIR} represents the flux emitted between 40 to 120 μm, and only for this part of the continuum do we claim that the emission is due to dust reradiation of starlight.

Additional supporting evidence for the thermal origin of the FIR emission in Seyferts comes from Fig. 3 where the ratio L_{IR}/M_{H_2} has been plotted as a function of the dust temperature T_d, where again the various symbols denote different classes of galaxies. Dust temperatures were derived from the ratio of $60/100$ μm flux densities and assuming an λ^{-1} emissivity law. All types of galaxies, Seyferts, starbursts, and the ULGs, show the same trend, ie, L_{IR}/M_{H_2} increases with increasing temperature. This can be easily explained on the grounds of dust models, because while the CO luminosity and $M(H_2)$ scale roughly linearly with temperature, L_{IR} scales as the 5-6 power of temperature. This is assuming an emissivity index in the range 1 to 2 (Sanders et al. 1991 find an emissivity index of 1.6 for their sample of luminous IRAS galaxies).

3.3. Comparison with observations of neutral hydrogen

A third argument in favour of the thermal origin of the FIR emission in Seyferts comes from comparisons of the CO line with observations of the HI λ21cm hydrogen line. In the following some of the most interesting cases are discussed in details, while Fig. 4 shows, for comparison, the CO and HI profiles.

NGC 7469 was observed in HI by Heckman et al. (1978). A prominent deep minimum is seen in the HI profile. However, the possibility that this minimum is an absorption feature was ruled out on the basis of the evidence that this absorption feature was equally prominent in the direction of IC 5283 which is a companion to NGC 7469. On the assumption of the validity of the previous claim the first main peak on the HI profile is similar to the CO profile measured here. The HI FWZI is 885 km/s, similar to the CO FWZI of 900 km/sec, while the similarity in the shapes of the line profiles imply that CO and HI are well mixed in the galaxy.

NGC 3227 is an interacting system galaxy. Mirabel & Wilson (1984) observed this galaxy in HI. The HI profile shows a prolonged plateau followed by a narrow emission peak. Our CO profile is a lot smoother with two CO peaks, one at 1089 km/sec and the other at 1257 km/sec. Our two component CO profile is consistent with the two intensity peaks in the interferometric observations of the same galaxy by Meixner et al. (1990). The HI peak was measured at 1146 km/sec, which is the value we have used to center our CO observations. Heckman et al. (1978) noted that their HI map made at Arecibo, shows evidence of interaction that might disturb the HI kinematics. Therefore, it is possible that some of the gas seen in their maps is related to the interaction between the two galaxies. The HI FWZI is 575

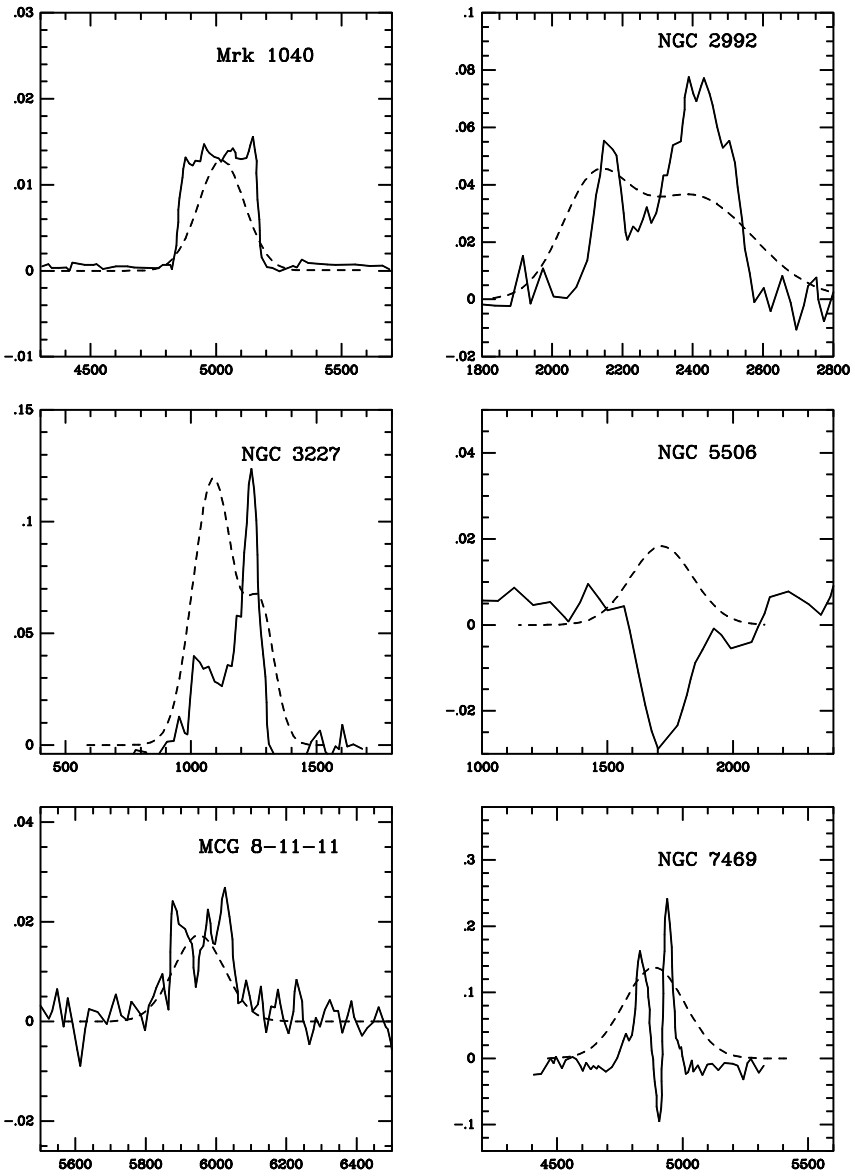

Fig. 4. HI line emission profiles (segmented line) superimposed on CO line emission profiles (straight line). The HI data for Mrk 1040, NGC 2992, and NGC 7469 come from Mirabel & Wilson (1984), for NGC 3227, NGC 4151 and MCG 8-11-11 from Heckman et al. (1978) and for NGC 5506 from Dickey (1982).

km/sec, while our two peaks have a FWZI of 500 and 400 km/sec for the strongest and the weakest respectively.

NGC 2992 is strongly interacting with NGC 2993. HI observations were carried out by Mirabel & Wilson (1984). The HI line has a total FWZI of 600 km/sec. The narrow HI peak at a higher velocity is probably related to the tidal tail to the north. The CO line profile is very flat topped and is well fit by two gaussians of unequal heights, one at 2128 and the other at 2395 km/sec. The flat-topped CO profile implies that the CO gas is concentrated in the inner parts of the galaxy. The HI and CO FWHM beamsizes are $3'.3$ and $23''$ respectively, therefore it is tempting to conclude that the emitting region must be of the order or smaller than $23'' = 5.35$ kpc in diameter, so most of the H_2 gas is located in the central parts of the galaxy.

Mrk 1040 = NGC 931 is another interacting galaxy. It shows a flat-topped HI emission line of almost 500 km/sec FWZI (Mirabel & Wilson 1984), which is quite distinct from our gaussian shaped CO emission line profile. Solid body rotation encompassing most of the optical disk could explain the observed 500 km/s HI width. The differences between the HI and CO profiles reveal the differences in the radial distribution of the HI and CO clouds.

MCG 8-11-11 was detected in HI emission with a FWZI line width of 450 km/sec. This compares well with the 500 km/sec CO FWZI, given that both detections are at 3σ level. There is also agreement in the profiles of the two emission lines.

NGC 4151 shows the same narrow line profile both in CO and HI emission. The FWZI of the HI emission line is almost 300 km/sec (Heckman et al. 1978) which actually matches well with our lower S/N detection with a FWZI of 250 km/sec.

NGC 5506 is an example of a galaxy where HI has also been detected in absorption (Thuan & Wadiak 1982, Dickey 1982). Since the width of the HI absorption line is only 48 ± 15 km/sec, it is difficult to draw any conclusions on whether this is due to

internal motions of the gas clouds near the active nucleus, or is originating from intervening clouds far from the active nuclei. NGC 5506 is an edge-on galaxy.

NGC 2110 was only marginally detected by Mirabel & Wilson (1984). For *NGC 7314, NGC 4593* only HI velocities and no emission line profiles were found in the literature while for *NGC 7172* no information on HI emission has been reported. The generally good agreement between the optically thin neutral hydrogen HI line and the optically thick CO line is consistent with the hypothesis that the FIR emission in AGNs is indeed due to star formation rather than the active galactic nucleus.

3.4. CO vs Nonthermal Radio Power

Rickard et al. (1985) and Stark et al. (1986) were among the first to comment on the relationship between CO luminosity and non-thermal radio continuum for galaxies. Based on CO (J= 1 → 0) observations of mostly Seyfert 2s and some Seyfert 1s and comparisons with a sample of non-Seyferts Heckman et al (1989) concluded that Seyfert galaxies have a higher non thermal radio power for a given CO luminosity. In Figs. 4 and 5 we have plotted the CO luminosities vs the non thermal 1.4 GHz radio power for the sample galaxies of the present study. In these plots we have only included objects with confirmed detections and no upper limits. The CO vs $P_{1.4GHz}$ relationship for Starbursts and ULGs is a tight one, in accordance with the Heckman et al. (1989) results. Using again the least squares bisector method we find that the linear regression between $logL_{CO}$ and $logP_{1.4GHz}$ is, $logL_{CO}$ = $(7.23 \pm 0.20) + (0.86 \pm 0.10)[logP_{1.4GHz} - 20]$ (in this case the normalisation, A, is the $logL_{CO}$ value at $logP_{1.4GHz}$ = 20).

The CO vs $P_{1.4GHz}$ correlation for the Seyferts is not as tight as that one for the starbursts. In this case the regression is $logL_{CO}$ = $(6.10 \pm 0.47) + (0.96 \pm 0.15)[logP_{1.4GHz} - 20]$. The slope of the regression line is consistent within errors for both Seyferts and starbursts plus ULGs, but the resulting best fit value of A in the case of the Seyferts is smaller than the best fit value of A for starbursts plus ULGs ($A_{Sy1+2} - A_{starburst+ULGs}$ = 1.13 ± 0.51). Furthermore, in Figs. 5 and 6 we have plotted the best fit regression line to the L_{CO} vs $logP_{1.4GHz}$ starburst+ULGs plot. Relative to this line, we find that 7 of the starburst plus ULGs lie to the upper left and 8 to the lower right while, for the Seyfert sample, only 3 lie to the upper left of the same line and 15 to the lower right. Using a χ^2 contingency table analysis, we find that the difference in these two distributions (Seyferts vs. starburst+ULGs) is significant at better than 99.8% confidence level. These results strongly suggest that there is a significant excess radio non thermal power at a given CO luminosity for the Seyfert sample. Note that this result holds for the Seyfert galaxies as a whole; as is obvious from Fig. 4, there is no difference between Seyfert 1 and Seyfert 2 in the L_{CO} vs $logP_{1.4GHz}$ relationship, both objects appear to have similar excess of nonthermal power for a given CO luminosity.

Finally, we investigated the relationship between 10μm emission and CO emission for the present sample of Seyfert galaxies. *No correlation was found between the two physical quantities*. We note that the 10μm emission is found to correlate well with the nuclear non-stellar NIR emission but less well with the IRAS 60μm emission and even worse with the IRAS 100μm emission (e.g. Giuricin et al. 1995). We stress that the mid- and far-IR components in Seyferts have distinct origins. The mid-IR is related to the AGN while the FIR component (as we have shown) is related to star formation activities. Our results, are in agreement with the work of de Grijp et al. (1985, 1987) who selected AGNs from the IRAS PSC based on their 25 μm data and the "warm" 60/25 colours.

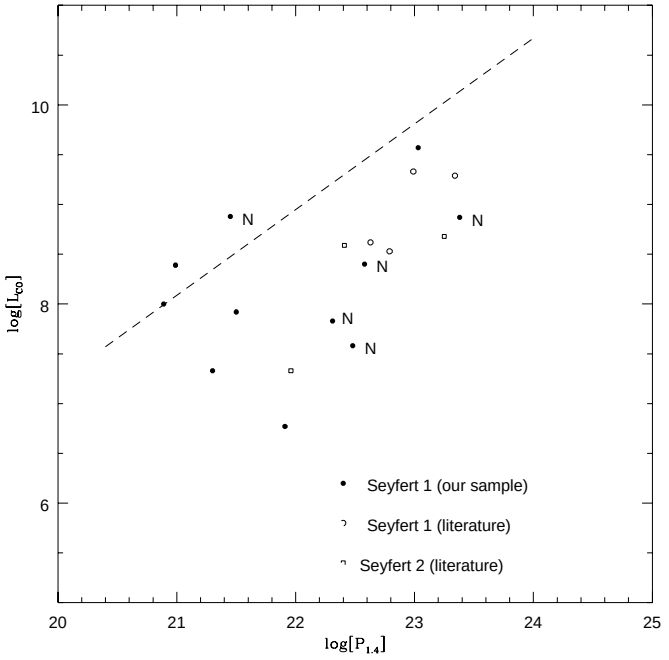

Fig. 5. The CO vs $P_{1.4GHz}$ relationship for the Seyfert galaxies. Solid circles are Seyfert 1s from our sample, open circles are Seyfert 1s from the literature and open squares are Seyfert 2s from the literature.

3.5. Investigating the differences between Sey 1, Sey 2 and NLXGs

So far, our discussion was mostly centered on the issue of the origin of the FIR emission from AGNs which we tried to investigate via its strong correlation with the CO emission. Here, we consider the differences (if any) between the two types of Seyfert activity. Heckman et al. (1989) has detected only a small number of Seyfert 1 galaxies, however, based on these observations they concluded that Seyfert 2s differ from Seyfert 1s in the strength of both their millimetre-wave CO and far-infrared continuum emission. They found that the molecular reservoir in Seyfert 2s is higher than that of Seyfert 1s, the latter more closely resemble normal field galaxies in their molecular properties.

From the Piccinotti sample (1982) studied here, we have obtained very good S/N observations for 6 Seyfert 1s and 5 NLXGs. Although our sample is small, it is still worth trying to investigate whether there are any differences in the CO and FIR

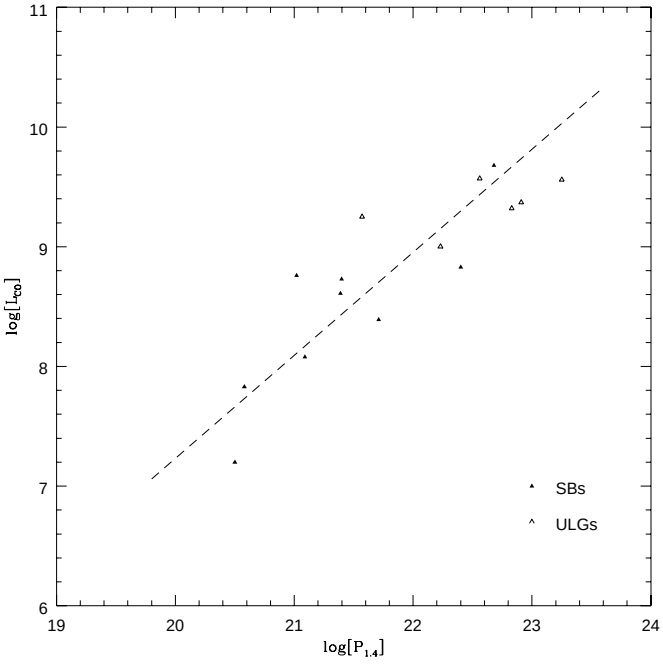

Fig. 6. The CO vs $P_{1.4GHz}$ relationship for the Starbursts (solid triangles) and ULGs (open triangles).

properties between the Seyfert 1s and NLXGs in it. In order to increase the number of objects under consideration, we include in our analysis the data for Seyfert 1 and 2 that we have collected from literature (as described in Sect. 3.2). As a result, the total number of Seyfert 1 that we consider is 10 (hereafter the T1 sample) and the number of Seyfert 2 is 8 (hereafter the T2 sample). Despite the fact that the objects in the T1 and T2 samples are selected according to rather an inhomogeneous way, as can be seen from Fig. 5, there is a good match in the distribution of 1.4 GHz radio continuum luminosity (which is a direct measure of intrinsic nuclear luminosity) between the objects in these samples. The mean radio power for the T1 and T2 samples is 22.34 and 22.22 respectively, almost identical for both of them. We can then reasonably assume that, although the number of objects in the T1 and T2 samples is not large, they nevertheless represent "fair" samples of the Seyfert population in the sense that they are not biased toward Type 1 or 2 objects.

The mean $\log(L_{CO})$ for the T1 and T2 samples is 8.28 and 7.85 respectively. The mean $\log(L_{FIR})$ for the same samples are 10.05 (T1 sample) and 10.53 (T2 sample) and, finally, the mean $\log(L_{FIR}/M(H_2)$ is 1.96 (T1 sample) and 1.84 (T2 sample). In all cases, using the Wilcoxon rank sum test, we find that the difference in the means is not statistically significance (ie at a significance level better than 5%). These results indicate that there are no significant differences in the FIR and/or CO emission between the objects in the T1 and T2 samples. This can be easily seen from Fig. 2, where there appears to be no difference in the $\log(L_{FIR})$ vs. $\log[M(H_2)]$ relationship of T1 and T2 objects (if we fit the linear model described in Sect. 3.2 to Seyfert 1 and 2s the best fit values for A are 8.33 ± 0.16 and 8.75 ± 0.38 for the T1 and T2 samples, and the best fit values for B are 1.18 ± 0.11 and 1.05 ± 0.27 for the two samples respectively, consistent within the errors in both cases). Furthermore, if Seyfert 2s had significantly higher FIR and CO emission they should occupy the upper left part of the plot, which is not the case.

4. Line profiles

The observed CO line profiles in external galaxies result from the convolution of the antenna beam pattern with the intrinsic emissivity distribution for which the velocity varies across the beam. Ideally, in order to trace the distribution of the CO gas one needs a very fine resolution which cannot always be achieved. However, for some galaxies there exist optical kinematic data with effective angular resolution much finer than that of CO. Under the assumption that the optical data also apply to the molecular clouds then one can use the velocity distribution in order to derive a higher resolution emissivity distribution which will best match the observed CO profiles.

In this section we attempt to study the distribution of CO clouds in our sample galaxies using optical kinematic data. Based on the exact knowledge of the rotation curves we have attempted to "reconstruct" the distribution of the CO gas. The current work was inspired from the first application of the so-called "deconvolution technique" on CO interferometric data from NGC 1068 by Scoville et al. (1983). This iterative rectification technique is used in order to derive the cloud distribution on a scale much smaller than the antenna resolution, by exploiting the spatial information implicit in the line profiles when the gas kinematics are known *a priori* (e.g. from optical line studies). For a detailed description of the technique the reader can refer to the Scoville et al. (1983) paper. For the computations we have assumed axisymmetrical density distribution. We have also adopted a Gaussian beam shape whose exact FWHM size varies for each of the galaxies studied. Since the emissivity distribution $\rho(R)$, is the unknown parameter, we have started off with the initial guess that it is being kept constant with radius. Rotation curves from optical line studies for 5 of our sample galaxies are available by Keel (1996). We note that for NGC 5506, which is a dusty edge-on galaxy, the optical data do not sample the real disk velocity field so we have not attempted to model this galaxy. Here, we present results for NGC 3227, NGC 7469 and MRK 1040. The results are shown in Fig. 7. In the left-hand side plots the observed and modelled line-spectra are shown (the thick line is the fitted model), while the right hand side panels show the density distribution along the radius of the galaxy. The rotation curves are not shown but can be found in Keel (1996).

NGC 3227 shows, according to Keel (1996), solid body rotation. For the deconvolution technique we adopted this velocity distribution and also a Gaussian beam shape with full width at half power of 4.84 Kpc on the sky. The dispersion parameter employed in the velocity broadening function was 16.25 km s^{-1}. Starting from an initial guess which was taken to be constant with radius, the procedure arrived at the distribution shown in Fig. 7 after 12 iterations. The density seems to peak at the center

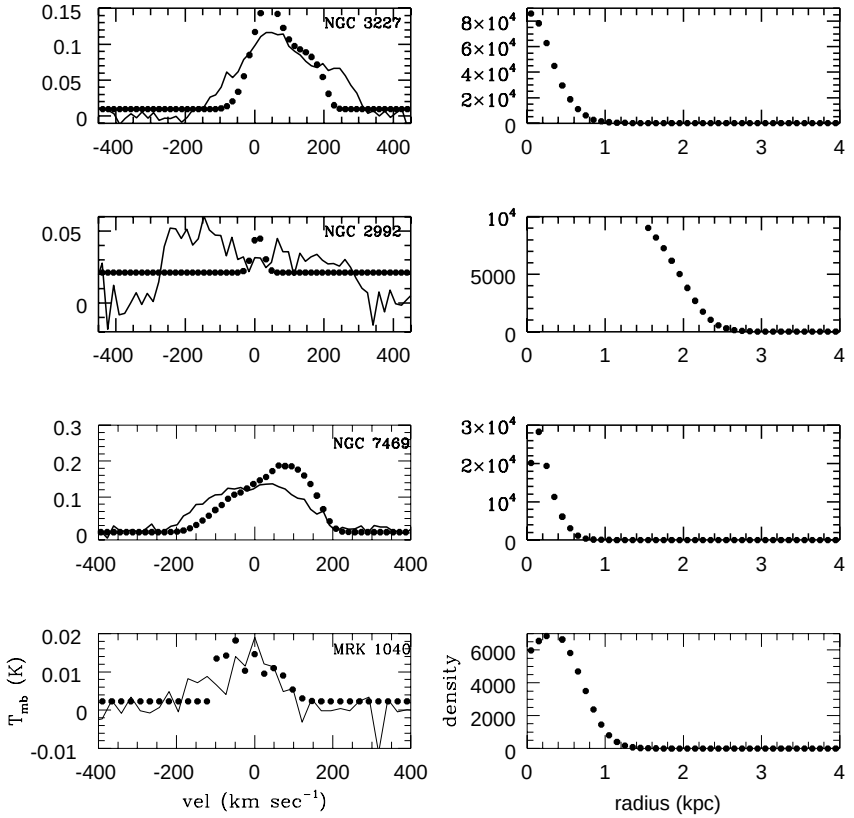

Fig. 7. Model line profiles (dotted line) compared with the observed emission for four galaxies, NGC 3227, NGC 2992, NGC 7469, MRK 1040. The right hand side plots the CO density distribution alonmg the radius (emissivity profiles) is shown.

of the galaxy and the CO clouds seem to be confined in the inner 1 kpc around the nucleus.

NGC 2992 has a peculiar rotation curve, denoted as 'distorted' by Keel (1996). Due probably to the low signal-to-noise ratio for this galaxy the fitted model does not agree well with the observed line profile. For the procedure we have used the same value for the velocity broadening function as before but a different value for the FWHP of the beam. The fit is rather poor (probably due to the large errors in our profiles) so we do not think that the derived cloud distribution of R$<$ 3 kpc is a realistic one.

The optical data for NGC 7469 show that the rotation curve rises rapidly from the nucleus to a flat plateau and is thus classified as a "normal rotation curve". Same parameters as in NGC 3227 were used for the procedure. The fit shown in Fig. 7 was reached after 9 iterations. The cloud distribution peaks at 0.2 kpc and extends out to about 1.0 kpc away from the center. NGC 7469 is known to have a starburst ring at a distance of 0.4 kpc away from the nucleus. It is interesting that the peak of the CO distribution is not at the center but at 0.2 kpc, indicating that there is "extended" CO structure. Although this technique didn't recover the exact distribution of the molecular clouds in NGC 7469, the fact that it did showed some structure at the 0.2 kpc area proves how useful the technique could be in tracing the CO distribution. Application of the rectification procedure at mapped CO data from NGC 7469 will probably resolve better the emission from the nucleus and the ring.

Finally, MRK 1040 shows a mixed solid body/normal rotation curve. The rectification technique provided us with a satisfactory fit and a rather puzzling distribution for the CO gas which peaks at R≈0.4 kpc instead of the very center of the galaxy. This very interesting result suggests that the clouds in MRK 1040 may form a ring rather than being concentrated in the nucleus of the galaxy. The ring interpretation is in accordance with the flat-topped CO profile of this galaxy.

Overall, the rectification technique seems to work better for galaxies with normal/solid body rotation curves. In all cases the clouds are distributed within the inner ≈1-1.5 kpc from the nucleus, with the exception perhaps of MRK 1040 where the distribution peaks at 0.4 Kpc away from the nucleus. We emphasize the need for yet more higher resolution optical data which can be used in conjunction with the rectification technique in order to trace the spatial distribution of the CO clouds in external galaxies.

5. Conclusions

We have presented high S/N detections of a sample of hard X-ray selected Seyfert galaxies. We have investigated the relation between CO and FIR luminosities and found that it follows the strong relation seen in normal and bright infrared galaxies. Our data confirm that the FIR emission in AGNs (especially type 1 Seyferts and NRLX galaxies) is of thermal origin and most probably is due to dust heated by starlight. It is stressed that in estimating FIR we took into account only the 60 and 100 μm

fluxes and not the 12 and 25 μm ones. As it was mentioned before (see Sect. 3.4) the 10 μm luminosity which has a strong nuclear component (e.g. Miley et al. 1985), correlates well with the 12 and 25 μm IRAS luminosities in AGNs (Giurcin et al. 1995) but much poorer with the 60 and 100 μm luminosities. Also no correlation was seen between CO and 10 μm emission. Of course one could still argue that the nuclear activity contributes to the 60 μm emission although we anticipate that the contribution is very small.

Recent results from ISO observations of a sample of Seyfert galaxies (Rodriguez-Espinosa et al., 1996) have shown that dust emission comes from two distinct regions: a warm dust component which peaks around 20 μm and a cold dust one peaking around 100 μm. According to these results emission from the first component is related to nuclear activity while the second dust component is related to star forming regions. So our result on the origin of the FIR emission in AGNs is in agreement with the ISO findings. That dust reradiation heated by starlight is the prime FIR mechanism in AGNs is also supported by the $L_{IR}/M(H_2)$ dependence on dust temperature as well as the similar shapes of HI and CO line profiles which actually implies that CO and HI gas are well mixed in these galaxies.

We have also investigated the relationship between CO and radio emission at 1.4 GHz. We found that Seyferts, when compared to starbursts and ULGs, show an excess radio nonthermal power at a given CO luminosity. This result is consistent with previous results (e.g. Heckman et al. 1989) and strongly suggests that, contrary to the FIR emission which is consistent with being fueled only by star formation, the radio continuum radiation in Seyferts has an extra component, most probably connected with nonthermal nuclear activity.

We found that there are no intrinsic differences in the CO and far-infrared properties between the type 1 Seyferts, type 2 Seyferts, and NLXGs studied here. They have the same average L_{FIR} and L_{CO}, and they follow the same L_{FIR} vs L_{CO} relationship. This result is in accordance with the notion that NLXGs are dust-rich versions of type 1 Seyfert galaxies. Our result also favours current unification theories according to which the classification of a Seyfert galaxy as type 1 or 2 depends solely on the direction from which it is viewed.

Finally, we have modelled the observed CO line profiles by means of the Scoville et al. "rectification technique". We have found that the molecular material is concentrated towards the center of the galaxies, within the inner 1-1.5 kpc with the exception of MRK 1040 for which the emissivity distribution peak at 0.4 kpc away from the nucleus implying the presence of a molecular ring. More optical data and yet interferometric CO studies will help to trace with even more accuracy the cloud distribution and kinematics of CO clouds in external galaxies.

Acknowledgements. We wish to thank Remo Tilanus and Chris Purton for their invaluable assistance during the remote observations of the present sample, Sarah Church for helping with the on-line data analysis and David Hughes for enlightening discussions on the subject. We thank the referee, Bill Keel for suggesting the rectification technique, and Nick Scoville for making the code available to us. DR acknowledges the support of the PPARC for a studentship and for the funding of millimetre and submillimetre astronomy in the UK.

References

Alloin D., Barvainis R., Gordon M.A., Antonucci R.R.J., 1992, A&A 265, 429
Blitz L., Mathieu R.D., Bally J., 1986, ApJ 311,142
Bloemen J.B.G.M., Strong A.W., Mayer-Hasselwander H.A., et al., 1986, A&A 154,25
Bregman J.N., 1990, ARA&A (2), 125, 20, 431
Casoli F., Dupraz C., Combes F., 1992, A&A 192, L17
Chini R., Krügel E. and Steppe H., 1992, A&A 255, 87
de Grijp M.H.K., Miley G.K., Lub J., de Jong T., 1985, Nat. 314,240
de Grijp, M.H.K., Miley, G.K., Lub, J., A&AS 70. 95
Dickey J.M., 1982, ApJ 300, 190
Giuricin G., Mardirossian F., and Mezzetti M., 1995, ApJ 446, 550
Heckman T.M., Balick B., Sullivan W.T., 1978, ApJ 224,745
Heckman T.M., Blitz L., Wilson A.S., Armus L., 1989, ApJ 342, 735
Helou G., Soifer B.T., Rowan-Robinson M., 1985, ApJ 298, L7
Ho L., Filippenko A.V., Sargent W.L.W., Peng C.Y., 1997, ApJS, submitted
Isobe T., Feigelson E.D., Akritas M.G., Babu G.J., 1990, ApJ, 364, 104
Keel W.C., 1996, AJ 111, 696
Krugel E., Steppe H. Chini R., 1992, A&A 229, 17
Maiolino R., Ruiz M., Rieke G.H., et al., 1997, ApJ in press
Matthews H.E., 1992, in The James Clerk Maxwell Telescope: A guide for the prospective User, JAC, Hilo, Hawaii
Mazzarella J.M., Graham J.R., Sanders D.B., Djorgovski S., 1993, ApJ 409, 170
Miley G.K., Neugebauer G., Soifer B.T., 1985, ApJ 293, 83
Mirabel I.F., Wilson A.S., 1984, ApJ 277,92
Meixner M., Puchalsky R., Blitz L., Wright M., Heckman T., 1990, ApJ 354, 158
Rickard J.J., Harvey P.M., 1984, AJ 89, 1520
Rickard J.J., Turner B.E., Palmer P.M., 1985 AJ 90,1175
Piccinotti G., Mushotzky R.F., Boldt E., et al., 1982, ApJ, 253, 485
Rigopoulou D., Lawrence A., White G.J., Rowan-Robinson M., Church S.E., 1996, A&A 305, 747
Rodriguez Espinosa J.M., Pirez Garcia A.M., Lemke D., Meisenheimer K., 1996, A&A 315, L129
Sanders D.B., Scoville N.Z., Soifer B.T. 1991, ApJ 370,158
Scoville N.Z., Young J.S., Lucy L.B., 1983, ApJ 270,443
Scoville N.Z., Sanders D.B., Sargent A.I., 1986, ApJ 311, L47
Stark A.A., Knapp G.R., Bally J., Wilson R.W., et al., 1986, ApJ 310, 660
Telesco C.M., 1988, ARA&A 26, 343
Thuan T.X., Wadiak J., 1982, ApJ 252, 125
Ulich B.L., Haas R.W., 1976, ApJS 30, 247
Young J.S., Schloerb F.P., Kenney J.D., Lord, S.D., 1986, ApJ 304, 443
Young J.S., Scoville N.Z. 1982, ApJ 258, 467

This article was processed by the author using Springer-Verlag LaTeX A&A style file *L-AA* version 3.